indicated, beads were preincubated in assay buffer containing 0.1 M lysine or 0.1 M arginine (pH 7.3, 1 h, RT) before addition of brain homogenate. Washing buffer also contained 0.1 M lysine or arginine. After each washing step, beads were collected using a magnetic particle concentrator (MPC, Dynal).

Beads were washed three times with 1 ml washing buffer (containing 2–6 M urea where appropriate) and once with 1 ml PBS by vortexing for 15 s at RT and collecting with the MPC. Finally, beads were sedimented by centrifugation (no other centrifugation steps were performed), supernatant was discarded, and loading buffer (24 μl) was added. The preparation was heated to 95 °C for 5 min. Samples were run immediately or stored at −20 °C, in which case they were reheated before loading.

Western blot analysis

Bead eluates (24 μl) or brain homogenates (12 μl) were run on SDS-PAGE (5% stacking and 12% resolving) and blotted on nitrocellulose membranes (Schleicher & Schuell). Membranes were blocked with 5% (w/v) nonfat dry milk (NDM) in Tris-buffered saline–Tween (TBS-T) at RT for 30 min, incubated with 12.5 ml TBS-T/1% NDM and 5 μg antibody 6H4 (Prionics, Zürich) at RT under agitation for 1 h, washed three times for 10 min in TBS-T, and incubated with 12.5 ml TBS-T containing 1% NDM and rabbit anti-mouse IgG1-horseradish peroxidase (Zymed, 1:10,000) at RT under agitation for 30 min. Membranes were washed three times for 15 min in TBS-T, and developed using enhanced chemuluminescence (ECL) detection reagents. Signals were recorded on film and/or quantified using a Kodak ImageStation.

Infectivity bioassay

Groups of 3–5 *tga20* transgenic mice were inoculated i.c. with 20 μl PBS containing 0.2% of the beads used for precipitation. Implantation of non-infectious beads did not induce clinical signs; histological examination revealed mild perifocal gliosis but no spongiosis. Incubation time until development of terminal scrapie sickness was determined, and total infectivity titres in beads used for precipitation were calculated[20] using the relationship $y = 12.63 - 0.088x$, where y is the ID_{50} and x is incubation time (days) to terminal disease[2].

Received 12 July; accepted 19 October 2000.

1. Prusiner, S. B. Novel proteinaceous infectious particles cause scrapie. *Science* **216,** 136–144 (1982).
2. Brandner, S. *et al.* Normal host prion protein necessary for scrapie-induced neurotoxicity. *Nature* **379,** 339–343 (1996).
3. Chen, Z. L. & Strickland, S. Neuronal death in the hippocampus is promoted by plasmin-catalyzed degradation of laminin. *Cell* **91,** 917–925 (1997).
4. Tsirka, S. E., Rogove, A. D. & Strickland, S. Neuronal cell death and tPA. *Nature* **384,** 123–124 (1996).
5. Büeler, H. R. *et al.* Normal development and behaviour of mice lacking the neuronal cell-surface PrP protein. *Nature* **356,** 577–582 (1992).
6. Korth, C. *et al.* Prion (PrP^{Sc})-specific epitope defined by a monoclonal antibody. *Nature* **390,** 74–77 (1997).
7. Prusiner, S. B. & Scott, M. R. Genetics of prions. *Annu. Rev. Genet.* **31,** 139–175 (1997).
8. Fischer, M. *et al.* Prion protein (PrP) with amino-proximal deletions restoring susceptibility of PrP knockout mice to scrapie. *EMBO J.* **15,** 1255–1264 (1996).
9. Riek, R. *et al.* NMR structure of the mouse prion protein domain Prp(121–231). *Nature* **382,** 180–182 (1996).
10. Riek, R., Hornemann, S., Wider, G., Glockshuber, R. & Wüthrich, K. NMR characterization of the full-length recombinant murine prion protein, mPrP(23–231). *FEBS Lett.* **413,** 282–288 (1997).
11. Shibuya, S., Higuchi, J., Shin, R. W., Tateishi, J. & Kitamoto, T. Protective prion protein polymorphisms against sporadic Creutzfeldt- Jakob disease. *Lancet* **351,** 419 (1998).
12. Zulianello, L. *et al.* Dominant-negative inhibition of prion formation diminished by deletion mutagenesis of the prion protein. *J. Virol.* **74,** 4351–4360 (2000).
13. Telling, G. C. *et al.* Prion propagation in mice expressing human and chimeric PrP transgenes implicates the interaction of cellular PrP with another protein. *Cell* **83,** 79–90 (1995).
14. Kaneko, K. *et al.* Evidence for protein X binding to a discontinuous epitope on the cellular prion protein during scrapie prion propagation. *Proc. Natl Acad. Sci. USA* **94,** 10069–10074 (1997).
15. Madani, R. *et al.* Enhanced hippocampal long-term potentiation and learning by increased neuronal expression of tissue-type plasminogen activator in transgenic mice. *EMBO J.* **18,** 3007–3012 (1999).
16. Baranes, D. *et al.* Tissue plasminogen activator contributes to the late phase of LTP and to synaptic growth in the hippocampal mossy fiber pathway. *Neuron* **21,** 813–825 (1998).
17. Ledesma, M. D. *et al.* Brain plasmin influences APP alpha-cleavage and Aβ degradation and is reduced in Alzheimer's disease brains. *EMBO Rep.* (in the press).
18. Naslavsky, N., Stein, R., Yanai, A., Friedlander, G. & Taraboulos, A. Characterization of detergent-insoluble complexes containing the cellular prion protein and its scrapie isoform. *J. Biol. Chem.* **272,** 6324–6331 (1997).
19. Houston, F., Foster, J. D., Chong, A., Hunter, N. & Bostock, C. J. Transmission of BSE by blood transfusion in sheep. *Lancet* **356,** 999–1000 (2000).
20. Prusiner, S. B. *et al.* Measurement of the scrapie agent using an incubation time interval assay. *Ann. Neurol.* **11,** 353–358 (1982).

Acknowledgements

We are grateful to D. Voelkel for providing fractionated human plasma, to P. Sonderegger, C. Weissmann, T. Lührs, and W. Schaffner for critical advice, and to M. Maissen and R. Hardegger for experimental help. This study was supported by grants from the European Union (Bundesamt für Bildung und Wissenschaft), the Swiss National Research Programs to A.A. and by a grant-in-aid of the SigmaXi foundation to M.B.F.

Correspondence and requests for materials should be addressed to A.A. (e-mail: adriano@pathol.unizh.ch).

Remission in models of type 1 diabetes by gene therapy using a single-chain insulin analogue

Hyun Chul Lee*†, Su-Jin Kim*†, Kyung-Sup Kim†‡, Hang-Cheol Shin* & Ji-Won Yoon*§

** Division of Endocrinology, Department of Internal Medicine; ‡ Institute of Genetic Science, Department of Biochemistry and Molecular Biology, Yonsei University, College of Medicine, Seoul 120–752, Korea*
§ Laboratory of Viral and Immunopathogenesis of Diabetes, Julia McFarlane Diabetes Research Centre, Department of Microbiology and Infectious Diseases, Faculty of Medicine, The University of Calgary, Calgary, Alberta T2N 4N1, Canada
† These authors contributed equally to the work.

A cure for diabetes has long been sought using several different approaches, including islet transplantation, regeneration of β cells and insulin gene therapy[1]. However, permanent remission of type 1 diabetes has not yet been satisfactorily achieved. The development of type 1 diabetes results from the almost total destruction of insulin-producing pancreatic β cells by autoimmune responses specific to β cells[2–6]. Standard insulin therapy may not maintain blood glucose concentrations within the relatively narrow range that occurs in the presence of normal pancreatic β cells[7]. We used a recombinant adeno-associated virus (rAAV) that expresses a single-chain insulin analogue (SIA), which possesses biologically active insulin activity without enzymatic conversion, under the control of hepatocyte-specific L-type pyruvate kinase (LPK) promoter, which regulates SIA expression in response to blood glucose levels. Here we show that SIA produced from the gene construct rAAV-LPK-SIA caused remission of diabetes in streptozotocin-induced diabetic rats and autoimmune diabetic mice for a prolonged time without any apparent side effects. This new SIA gene therapy may have potential therapeutic value for the cure of autoimmune diabetes in humans.

First, we generated SIA by replacing 35 residues of the C-peptide with a short turn-forming heptapeptide (Gly-Gly-Gly-Pro-Gly-Lys-Arg). We produced recombinant SIA in *Escherichia coli*, folded it and examined its biological activity. We found that the *in vitro* receptor binding and glucose uptake activity and the *in vivo* hypoglycaemic effect of SIA were substantially greater than that of proinsulin, but slightly lower than insulin, indicating that the biological activity of SIA is comparable to that of insulin (Table 1).

Second, we constructed a recombinant plasmid, pLPK-SIA

Table 1 Functional properties of the recombinant single-chain insulin analogue

	Insulin receptor binding* (ED_{50} in nM)	Glucose uptake† (ED_{50} in nM)	*In vivo* hypoglycaemic effect‡ (ED_{50} in nmol kg^{-1})	
			1 hour	2 hours
Human insulin	0.742 (100%)§	0.322 (100%)	1.5 ± 0.34 (100%)	1.8 ± 0.37 (100%)
Human proinsulin	36.1 (2%)	26.5 (1.25%)	9.1 ± 1.12 (16.5%)	9.6 ± 1.28 (18.8%)
Single-chain insulin analogue (SIA)	2.68 (27.7%)	1.56 (21.3%)	3.6 ± 0.42 (41.6%)	3.4 ± 0.18 (52.9%)

* ED_{50} values are presented as the concentration of unlabelled insulin or analogues required to decrease tracer insulin binding to 50% of maximal.
† ED_{50} values are presented as the concentration of insulin or analogues resulting in half-maximal glucose uptake rate.
‡ ED_{50} values are presented as the dose of insulin or analogues that gave half of the maximal hypoglycaemic activity 1 or 2 h after subcutaneous administration to fasted rats.
§ The percentage of proinsulin and SIA were determined on the basis of the ED_{50} value of human insulin as 100%.

(Fig. 1a) by cloning the SIA gene under the LPK promoter[8–12]. The albumin leader sequence was added to the frame of the SIA gene construct to facilitate the secretion of SIA from the hepatocytes, and the simian virus 40 (SV40) enhancer was added downstream of the *SIA* gene in order to elevate the basal level of SIA expression. When we administered pLPK-SIA into the portal vein of streptozotocin (STZ)-induced diabetic SD rats, we found that the blood glucose levels gradually decreased until the fifth day after administration, remained in a normoglycaemic state for an additional four days and gradually rose thereafter to reach over 500 mg dl^{-1} at 14 days after treatment. In contrast, STZ-induced diabetic rats treated with the pSIA construct without LPK remained hyperglycaemic (Fig. 1b). When we determined the presence of SIA DNA and mRNA in the liver, kidney, spleen, lung and heart five days after plasmid administration, we found that the transfected plasmid DNA was detected in only liver cells from both groups of rats, whereas SIA mRNA was expressed in only the pLPK-SIA-treated rats (Fig. 1c).

Third, we attempted to overcome the short half-life of the transfected DNA using an adeno-associated virus (AAV) vector, which is a safe and efficient gene delivery system[13,14] that integrates into the host chromosomal DNA in a site-specific manner[15–17]. We produced recombinant AAV containing the LPK promoter-SIA DNA (rAAV-LPK-SIA) in 293 cells. To determine whether rAAV-LPK-SIA can remit diabetes, we administered 10^{11} particles per animal through the portal vein of STZ-induced diabetic SD rats. The blood glucose levels gradually decreased in the rAAV-LPK-SIA-treated rats, reached the level of normoglycaemia one week after treatment and remained in a normoglycaemic state for more than eight months (Fig. 2a). However, lower doses of rAAV-LPK-SIA (10^9–10^{10} virus particles) were insufficient for complete remission. Higher doses of rAAV-LPK-SIA (10^{12} virus particles per rat) did not result in hypoglycaemia in the treated rats (Fig. 2a).

We then examined the molecular state of the rAAV genome in the liver of the recipients by Southern blots of liver DNA with SIA complementary DNA and the SV40 sequence as a probe. We found that rAAV-LPK-SIA DNA existed in both single-stranded and double-stranded states at the early stage (5 days) after the treatment, but only in the double-stranded state at later stages (5–25 weeks). In addition, we found that rAAV-LPK-SIA-DNA was integrated into the hepatocyte chromosomal DNA in a head-to-tail concatemeric manner at 25 weeks after treatment (Fig. 2b). These results indicate that the single-stranded recombinant adeno-associated viral genome is converted to a double-stranded genome in the infected hepatocytes and integrated into the chromosomal DNA.

We examined the localization of SIA expression in the liver by anti-SIA antibody staining, and found that SIA was expressed in the hepatocytes of rats treated with rAAV-LPK-SIA (Fig. 3a), but not in untreated control rats (Fig. 3b). SIA-expressing cells were clustered around the central vein and portal triads in the liver (Fig. 3a). Histological examination of the infected liver sections revealed no detectable damage (Fig. 3c and d). In addition, we found no difference in the level of plasma aspartate transaminase (AST) or plasma alanine transaminase (ALT), marker enzymes for hepatic damage, between saline-treated, normal control rats (94 ± 12 IU l^{-1} for AST and 46 ± 9 IU l^{-1} for ALT; $n = 5$) and rAAV-LPK-SIA-treated rats (95 ± 10 IU l^{-1} for AST and 40 ± 9 IU l^{-1} for ALT). Furthermore, we did not find anti-SIA antibody in the sera of the treated rats during the experimental period (data not shown). These results indicate that treatment of diabetic rats with rAAV-LPK-SIA resulted in the remission of diabetes without any apparent change in the infected liver cells or any adverse effects of SIA expression on the hepatocytes.

We questioned whether the remission of diabetes might be due to the secretion of insulin from residual pancreatic β cells in the STZ-

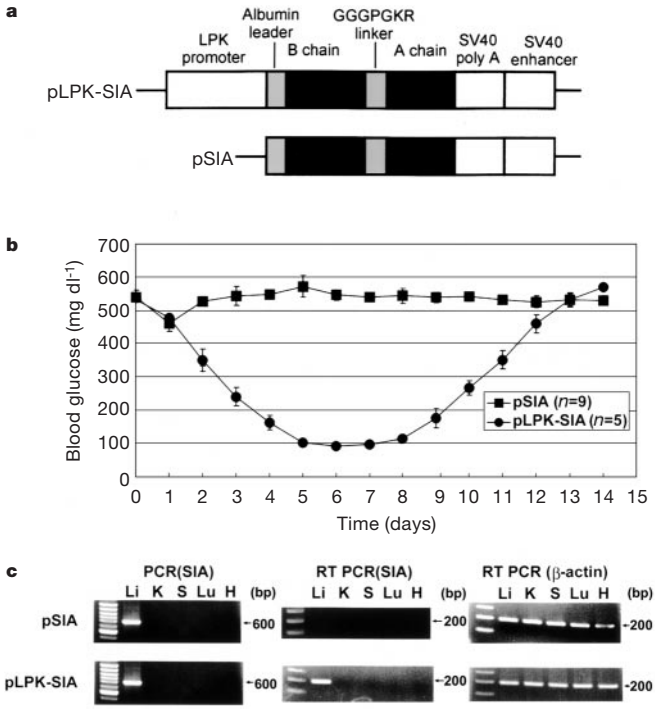

Figure 1 Construction of pLPK-SIA, hypoglycaemic effect of pLPK-SIA and hepatocyte-specific expression of pLPK-SIA. **a**, Diagram of pLPK-SIA and pSIA. **b,** Blood glucose levels in diabetic rats injected with pSIA or pLPK-SIA (mean ± standard deviation, s.d.). **c,** SIA DNA (left), SIA RNA (centre) or β-actin RNA as an internal control (right) in the liver (Li), kidney (K), spleen (S), lung (Lu) and heart (H) of rats 5 days after treatment with pSIA or pLPK-SIA. bp, base pairs.

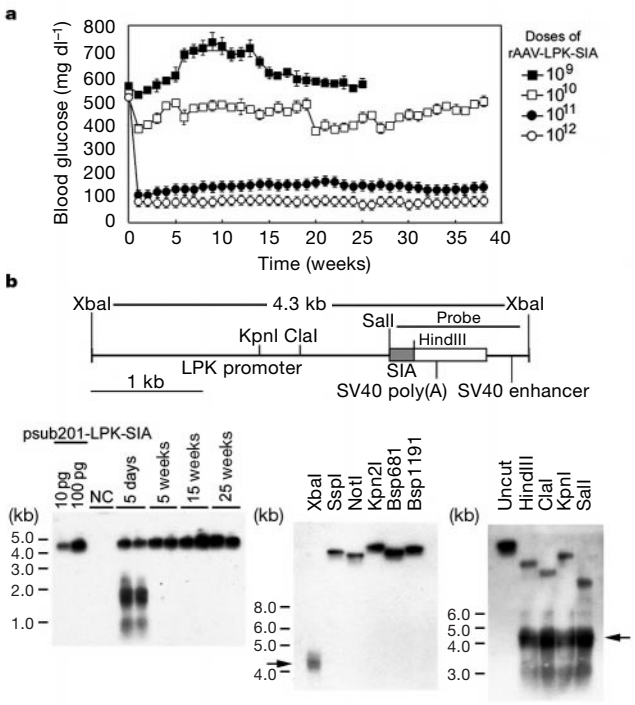

Figure 2 Hypoglycaemic effect of rAAV-LPK-SIA and integration of rAAV-LPK-SIA DNA into hepatocyte DNA. **a,** Blood glucose levels in STZ-induced diabetic SD rats ($n = 10$ per group) after injection of different doses of rAAV-LPK-SIA (mean ± s.d. value). **b**, Restriction enzyme map of LPK-SIA and the region used as a probe for Southern blots (top). Southern blot hybridization of liver DNA from rats treated with rAAV-LPK-SIA after digestion with *Xba*I at different times after treatment (left) and digestion with non-cutting (centre) or single cutting (right) enzymes at 25 weeks after treatment. *Xba*I-digested psub 201-LPK-SIA and liver DNA from normal SD rats (NC) were used as controls; arrows, 4.3-kb band.

treated rats, rather than the expression of SIA. We stained islets of rAAV-LPK-SIA-treated rats with anti-insulin antibody, and found that insulin-producing β cells were rarely seen in these islets (Fig. 3e), whereas insulin-producing β cells were clearly detected in normal control islets (Fig. 3f). In contrast, SIA was continuously produced for over 8 months after the treatment with rAAV-LPK-SIA (Fig. 3g; data after 25 weeks not shown). In addition, a negligible amount of C-peptide was found in plasma of the rAAV-LPK-SIA-treated rats after glucose loading (Fig. 3h). These results indicate that the control of blood glucose in rAAV-LPK-SIA-treated rats was not due to endogenous pancreatic insulin, but to the expression of SIA in the liver cells.

Fourth, we questioned whether the expression of SIA is truly regulated by blood glucose levels through the LPK promoter. We maintained different levels of blood glucose (approximately 100, 300 or 500 mg dl^{-1}) by a hyperglycaemic clamp method[18] for 30 min in rats in which the blood glucose had been normalized after treatment with 10^{11} particles of rAAV-LPK-SIA, and examined the production of SIA in the hepatocytes and plasma four hours after glucose loading. We found that the level of SIA expression was closely correlated with the concentration of blood glucose (Fig. 4b and c), even though similar levels of SIA DNA were found among the different groups of rats (Fig. 4a), indicating that the expression of SIA under the LPK promoter is properly controlled by blood glucose levels.

We next determined whether rAAV-LPK-SIA-treated rats (15–17 weeks old) clear glucose from the blood in a manner similar to non-diabetic normal rats by glucose tolerance tests (GTTs; Fig. 4d). We injected glucose (2 g per kg body weight intraperitoneally (i.p.), after 4 h of fasting) into rats treated with rAAV-LPK-SIA that had recovered from diabetes or normal, untreated rats and examined the plasma insulin or SIA levels and blood glucose concentrations after glucose loading. We found that the plasma insulin levels of normal rats peaked within 30 min and returned to basal levels at 2 h after glucose loading (Fig. 4e). However, the plasma SIA levels of rAAV-LPK-SIA-treated rats were delayed, peaking at 3–4 h and returning to basal levels at 6 h after glucose loading (Fig. 4e and f). The expression of SIA mRNA in the hepatocytes showed a similar pattern to that of plasma SIA (Fig. 4g). This difference in kinetics between insulin and SIA in response to glucose loading is probably due to the fact that insulin is rapidly released into the blood by exocytosis from the pancreatic β cells, which are highly sensitive to small changes in extracellular glucose. In contrast, the secretion of SIA is controlled at the transcriptional level by the LPK promoter;

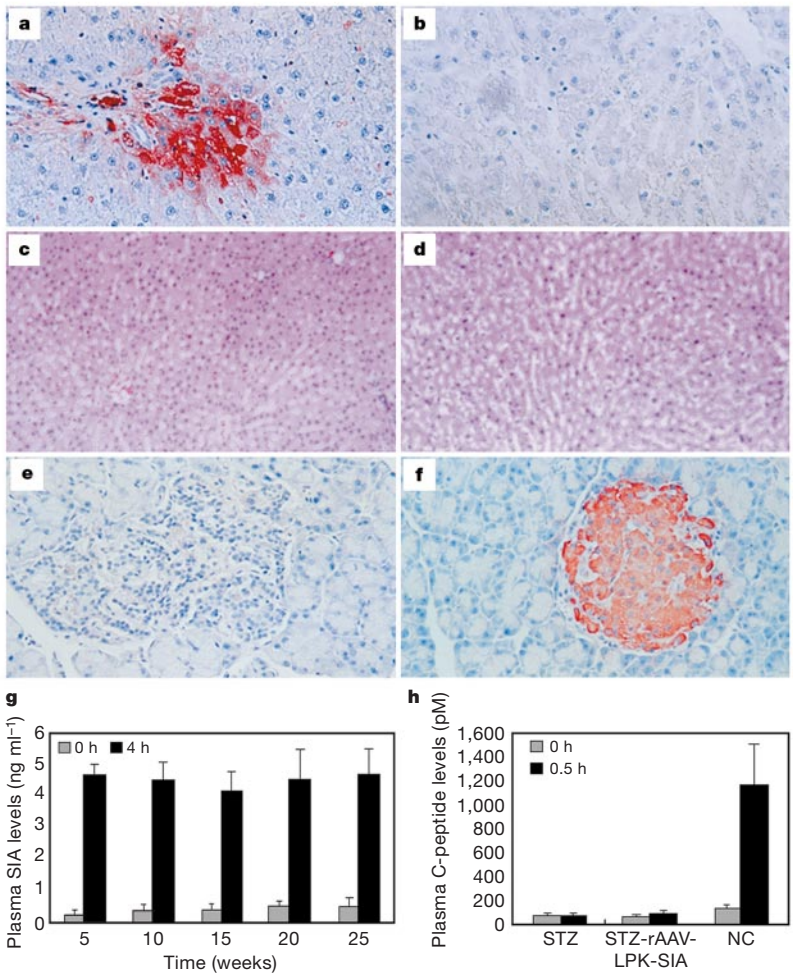

Figure 3 Expression of SIA in hepatocytes and plasma of rAAV-LPK-SIA-treated rats. Anti-SIA antibody staining of liver sections from **a,** rAAV-LPK-SIA-treated rats at 1 month after treatment and **b**, normal control rats. Haematoxylin and eosin (HE) staining of liver tissue from **c,** rAAV-LPK-SIA-treated rats and **d,** normal control rats. Anti-insulin antibody staining of pancreatic islets from **e,** rAAV-LPK-SIA-treated rats and **f,** normal control rats. **g,** Plasma SIA levels at 0 and 4 h after glucose loading in rAAV-LPK-SIA-treated rats ($n = 7$ per group). **h,** Plasma C-peptide levels at 0 and 0.5 h after glucose loading at 25 weeks after rAAV-LPK-SIA treatment (STZ-rAAV-LPK-SIA; $n = 7$). Normal nondiabetic rats (NC; $n = 7$) and untreated STZ-induced diabetic rats (STZ; $n = 7$); mean ± s.d.

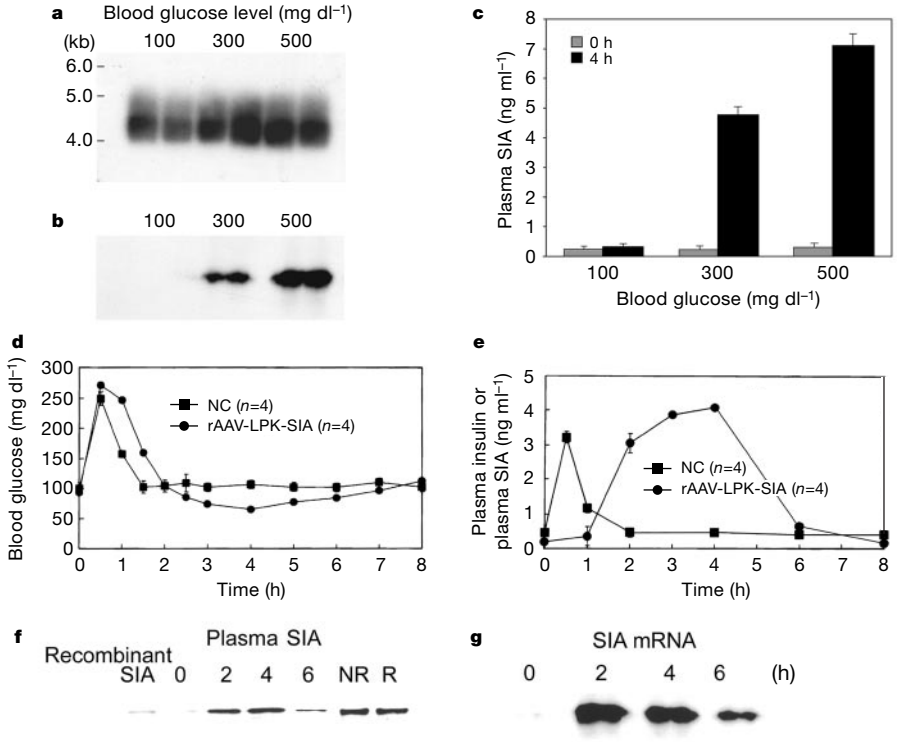

Figure 4 Response of SIA to glucose in rAAV-LPK-SIA-treated STZ-induced diabetic rats. **a,** Presence of SIA DNA and **b,** expression of SIA in the hepatocytes, and **c,** production of SIA in the plasma (n = 7 per group) after the maintenance of different blood glucose levels at 30 weeks after treatment with rAAV-LPK-SIA. **d**, Glucose and **e**, insulin or SIA levels during GTTs performed 4 weeks after treatment. NC indicates normal control rats; rAAV-LPK-SIA indicates rats treated with rAAV-LPK-SIA (mean ± s.d.). **f**, Western blots of plasma SIA at the indicated times (h) after glucose loading. NR, non-reducing condition; R, reducing condition. **g**, Expression of SIA mRNA after glucose loading examined by RNase protection assay.

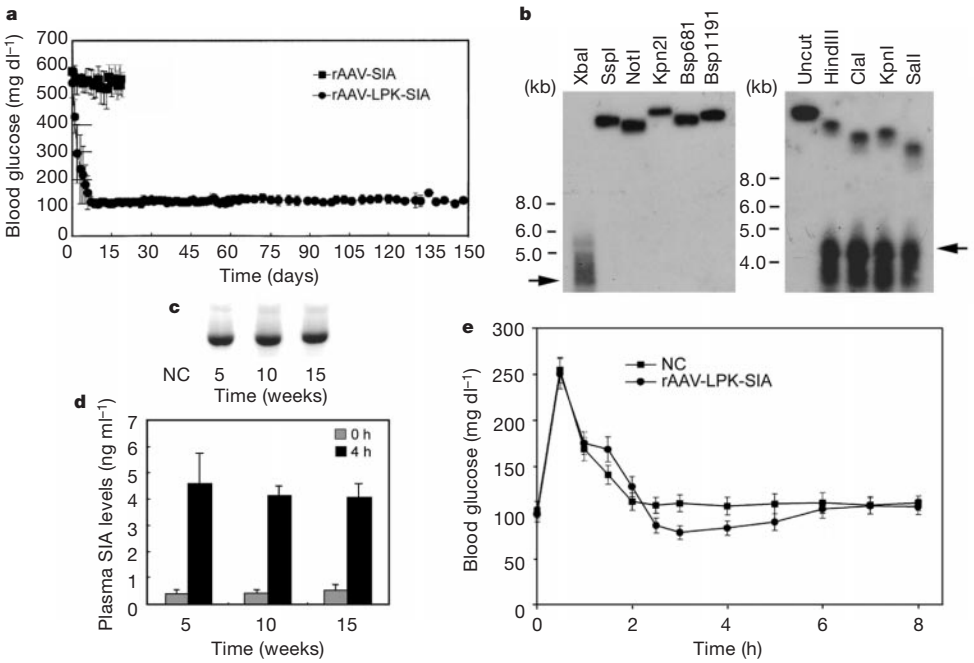

Figure 5 Remission of autoimmune diabetes in NOD mice by administration of rAAV-LPK-SIA. **a,** Blood glucose levels in diabetic NOD mice after rAAV-SIA or rAAV-LPK-SIA treatment ($n = 6$ per group). **b,** Integration of SIA DNA into hepatocyte DNA analysed by Southern blot at 15 weeks after rAAV-LPK-SIA treatment (arrows, 4.3-kb band). **c,** SIA mRNA in hepatocytes (NC, untreated NOD mice) and **d**, plasma SIA at 0 and 4 h after glucose loading at various times after treatment ($n = 5$ per group). **e,** Blood glucose levels during GTTs in rAAV-LPK-SIA-treated NOD mice ($n = 5$) and control NOR mice (NC, $n = 7$); mean ± s.d.

thus a prolonged period is required to change the plasma SIA level in response to blood glucose.

In these GTTs, we found that the blood glucose levels of normal rats peaked at 30 min after glucose loading, returned to the normal range (around 100 mg dl^{-1}) at 90 min, and stabilized thereafter (Fig. 4d). The blood glucose levels of rats treated with rAAV-LPK-SIA showed a similar pattern to normal rats, except for a slightly delayed time to recover normal glucose levels (120 min versus 90 min) and transiently lower blood glucose levels from 3 to 6 h after glucose loading (Fig. 4d). Although the time required for plasma SIA levels to peak was delayed by 3.5 h, as compared to insulin, the recovery to normoglycaemia was only delayed by 30 min, as compared to the normal controls. This result indicates that the action of SIA on blood glucose levels began when SIA concentrations were rising during the first hour after glucose loading; thus the rising levels of SIA and the falling levels of blood glucose to normoglycaemia are well correlated within the first 2 h. The subsequent elevation of SIA from 2 to 5 h did not result in significant hypoglycaemia. We speculate that this may be due to a reduction in glucose sensitivity to SIA when the blood glucose levels are normalized, a reduction of the sensitivity of the post-receptor signal cascade during the period of high SIA levels, and/or compensatory increases in glucagon and catecholamines, which can increase blood glucose.

Fifth, we attempted to find whether rAAV-LPK-SIA can also cause remission of autoimmune diabetes in non-obese diabetic (NOD) mice. When we administered rAAV-LPK-SIA (10^{12} virus particles per mouse) to diabetic NOD mice, we found that the blood glucose levels reached normoglycaemia at seven days after treatment and remained in a normoglycaemic state for more than five months. In contrast, diabetic NOD mice treated with rAAV-SIA (without the LPK promoter) remained hyperglycaemic and died within three weeks (Fig. 5a). When we examined the presence of the SIA gene in the hepatocytes of NOD mice at 15 weeks after treatment with rAAV-LPK-SIA, we found that SIA DNA was integrated into the chromosomal DNA (Fig. 5b). We then examined SIA expression in the liver and plasma of the mice after glucose loading at 5, 10, and 15 weeks after treatment with rAAV-LPK-SIA, and found that SIA mRNA was clearly expressed (Fig. 5c) and SIA protein was released in the plasma (Fig. 5d). Anti-SIA antibody was not detected in the sera from these mice during the five months after treatment (data not shown). In addition, we performed GTTs in NOD mice that had recovered from diabetes. We found that the blood glucose levels of NOD mice treated with rAAV-LPK-SIA peaked at 30 min after glucose loading, returned to the normal range (115 mg dl^{-1}) at 120 min and stabilized thereafter (Fig. 5e). The time to recover normal blood glucose levels was slightly delayed and the blood glucose levels from 3 to 6 hours after glucose loading were slightly lower compared with normal non-obese diabetes-resistant (NOR) mice, similar to the pattern seen in the rats treated with rAAV-LPK-SIA.

We have developed a potential method for the treatment of autoimmune type 1 diabetes by the expression of a single-chain insulin analogue in the hepatocytes under the control of a hepatocyte-specific glucose regulatable promoter and SV40 enhancer. The host's cell-mediated autoimmune responses do not attack the SIA-expressing hepatocytes, resulting in long-term remission of autoimmune diabetes in NOD mice. The treatment of both chemically induced diabetes in rats and autoimmune diabetes in NOD mice with rAAV expressing the insulin analogue resulted in the permanent remission of type 1 diabetes without any detectable adverse effect on the hepatocytes. □

Methods

Cloning and expression of single-chain insulin analogue cDNA in *E. coli*

SIA cDNA was generated by polymerase chain reaction (PCR) using five overlapping oligonucleotides of 65–68 bases in length. The resulting SIA cDNA sequence was:

ATG/TTC/GTT/AAT/CAG/CAC/CTG/TGC/GGC/TCT/CAC/CTG/GTA/GAA/GCT/CTG/TAC/CTG/GTT/TGC/GGT/GAA/CGT/GGT/TTT/TTC/TAC/ACC/CCG/AAA/ACC/GGT/GGT/GGT/CCG/GGT/AAA/CGT/GGC/ATC/GTT/GAA/CAA/TGC/TGT/ACT/AGC/ATC/TGC/TCT/CTC/TAC/CAG/CTG/GAG/AAC/TAT/TGT/AAC/TAG/TAA.

The amino-terminal pentapeptide sequence (PSDKP) of TNF-α was added as a fusion partner. Ten histidine residues for convenience in the purification process and a methionine residue for chemical cleavage were inserted between the PSDKP sequence and SIA, then cloned into pET-3a[19] under the T7 promoter (pET-SIA). The fused SIA protein was expressed in *E. coli* BL21 (DE3) as inclusion bodies. The fusion protein was sulphonated at the cysteine residues and cleaved by CNBr treatment. S-sulphonated SIA was purified by cation-exchange chromatography (Pharmacia Biotech), refolded with β-mercaptoethanol and analysed by reverse-phase HPLC.

Examination of functional activity of recombinant SIA produced in *E. coli*

Insulin receptor binding and glucose uptake assays were performed using IM-9 lymphocytes as described previously[20–22]. To determine the *in vivo* hypoglycaemic activity of SIA, 8–10-week-old male Sprague–Dawley rats were fasted, and SIA protein (4–80 μg in 0.1 ml saline per 100 g body weight) or the same volume of saline as a control was injected subcutaneously[23]. Blood was obtained from the tail vein of each rat, and the glucose level was determined.

Construction of pSIA and pLPK-SIA

The SIA cDNA from pET-SIA was subcloned into the PCR-script (Stratagene) at the *Bam*HI/*Hin*dIII site. The SV40 poly(A) signal sequence from pCDM8 (Invitrogen) and the SV40 enhancer from the pGL3 (Promega) were amplified by PCR and subcloned at the *Hin*dIII/*Apa*I and *Apa*I sites, respectively. The albumin leader sequence (72 base pairs) was inserted in front of the SIA cDNA using a ExSite PCR-based Site-Directed Mutagenesis Kit (Stratagene). The clone containing the albumin leader sequence was isolated and designated as pSIA. The final construct, pLPK-SIA, was generated by insertion of the promoter of the rat LPK gene (−3193 to +18) amplified by PCR into pSIA at the *Xba*I/*Sal*I site.

Administration of pSIA, pLPK-SIA, rAAV-SIA or rAAV-LPK-SIA into the liver

Animals were anaesthetized with Ketamine-chloride (10 mg kg^{-1}). A midline abdominal incision was made, and a mixture of 30 μg of DNA-FuGENE 6 (Boehringer Mannheim) and rAAV-SIA or rAAV-LPK-SIA (10^9–10^{12} virus particles) was injected into the hepatic portal vein of animals that had been hyperglycaemic for 2 weeks.

PCR and PCR after reverse transcription of RNA

PCR was performed using the sense primers derived from the T7 or LPK promoter region (5′-GTAATACGACTCACTATAG GGC-3′ for pSIA-injected rats; 5′-ATTTCGAATAAG AAGAGGAAGGGAAG-3′ for rats injected with pLPK-SIA) and the antisense primers derived from the 3′ terminus of the SIA gene (5′-GCGCAAGCTTTTACTAGTTACAAT AGTT-3′). To detect SIA mRNA, the total RNA was isolated from various tissues and RT-PCR was performed using the primers 5′-GCGCGGATCCATGTTCGTTAATCAGCAC-3′ and 5′-GCGCAAGCTTTTACTAGTTACAATAGTT-3′. β-actin mRNA was amplified as an internal control.

Production of recombinant AAV-SIA and AAV-LPK-SIA

The 4.3-kilobase LPK-SIA including the SV40 enhancer was amplified by PCR from the pLPK-SIA plasmid and subcloned into psub201 at the *Xba*I site (psub201-LPK-SIA). The recombinant AAV (rAAV-LPK-SIA) was produced and purified as described previously[13–15]. The psub 201-SIA (without LPK) was used for the construction of rAAV-SIA. The amount of viral DNA was quantified by competitive PCR[14].

Southern blot analysis

Liver DNA (10 μg) was digested with various restriction enzymes. After agarose gel electrophoresis, the DNA was transferred to a membrane, hybridized with a ^{32}P-labelled probe containing the SIA cDNA and SV40 sequence, and detected by autoradiography.

Measurement of plasma insulin, C-peptide and SIA and blood glucose

Plasma insulin and C-peptide levels were measured using the Linco rat insulin RIA kit and Linco rat C-peptide RIA kit, respectively (Linco Research Immunoassay). For measurement of plasma SIA levels, we performed competitive ELISA using rabbit polyclonal anti-SIA antibodies. Blood glucose levels were measured as described elsewhere[24].

Hyperglycaemic clamp experiment

A 20% glucose solution, for maintenance of blood glucose at about 300 or 500 mg dl^{-1}, or saline, for maintenance of blood glucose at about 100 mg dl^{-1}, was perfused into the femoral vein using an electronic digital syringe pump (Harvard)[18]. The infusion rate was adjusted to maintain the desired blood glucose levels for 30 min. The production of SIA in the hepatocytes and plasma was examined 4 h later.

Western blot analysis

Proteins below 30,000 daltons were separated and concentrated from 1.5 ml of pooled plasma at 0, 2, 4 and 6 h. The proteins, with or without β-mercaptoethanol treatment, were electrophoretically separated on a 10–20% Tricine gradient gel (NOVEX). Western blot analysis was performed using rabbit polyclonal anti-SIA antibody.

RNase protection assay

10 μg of liver RNA was used for RNase protection analysis with ^{32}P-labelled SIA antisense RNA made from pET-SIA by *in vitro* transcription using T7 RNA polymerase.

Measurement of AST and ALT

AST and ALT were measured in an autochemical analyser (Hitachi 747) using an ultraviolet assay method[25].

Histological and immunohistochemical analysis

Sections of liver and pancreas were histologically examined[26,27] and stained with anti-SIA or anti-insulin antibodies, respectively[27,28].

Received 7 August; accepted 9 October 2000.

1. Levine, F. & Leibowitz, G. Towards gene therapy of diabetes mellitus. *Mol. Med. Today* **5,** 165–171 (1999).
2. Yoon, J. W. & Jun, H. S. in *Encyclopedia of Immunology* (eds Roitt, I. M. & Delves, P. J.) 2nd edn, 1390–1398 (Academic, London, 1998).
3. Schranz, D. B. & Lernmark, A. Immunology in diabetes: an update. *Diab. Metab. Rev.* **14,** 3–29 (1998).
4. Tisch, R. & McDevitt, H. Insulin-dependent diabetes mellitus. *Cell* **85,** 291–297 (1996).
5. Bach, J. F. Insulin-dependent diabetes mellitus as a β cell targeted disease of immunoregulation. *J. Autoimmun.* **8,** 439–463 (1995).
6. Rossini, A. A., Greiner, D. L., Friedman, H. P. & Mordes, J. P. Immunopathogenesis of diabetes mellitus. *Diabetes Rev.* **1,** 43–75 (1993).
7. The Diabetes Control and Complications Trial Research Group. The effect of intensive treatment of diabetes on the development and progression of long-term complications in insulin-dependent diabetes mellitus. *New Engl. J. Med.* **329,** 977–986 (1993).
8. Cuif, M. H., Doiron, B. & Kahn, A. Insulin and cyclic AMP act at different levels on transcription of the L-type pyruvate kinase gene. *FEBS Lett.* **417,** 81–84 (1997).
9. Chen, R., Doiron, B. & Kahn, A. Glucose responsiveness of a reporter gene transduced into hepatocytic cells using a retroviral vector. *FEBS Lett.* **365,** 223–226 (1995).
10. Decaux, J. F., Antoine, B. & Kahn, A. Regulation of the expression of the L-type pyruvate kinase gene in adult rat hepatocytes in primary culture. *J. Biol. Chem.* **264,** 11584–11590 (1989).
11. Cuif, M. H., Porteu, A., Kahn, A. & Vaulont, S. Exploration of a liver-specific, glucose/insulin-responsive promoter in transgenic mice. *J. Biol. Chem.* **268,** 13769–13772 (1993).
12. Bergot, M. O., Diaz-Guerra, M. J., Puzenat, N., Raymondjean, M. & Kahn, A. Cis-regulation of the L-type pyruvate kinase gene promoter by glucose, insulin and cyclic AMP. *Nucleic Acids Res.* **20,** 1871–1877 (1992).
13. Muzyczka, N. Use of adeno-associated virus as a general transduction vector for mammalian cells. *Curr. Top. Microbiol. Immunol.* **158,** 97–129 (1992).
14. Clark, K. R., Liu, X., McGrath, J. P. & Johnson, P. R. Highly purified recombinant adeno-associated virus vectors are biologically active and free of detectable helper and wild-type viruses. *Hum. Gene Ther.* **10,** 1031–1039 (1999).
15. Samulski, R. J. Adeno-associated virus: integration at a specific chromosomal locus. *Curr. Opin. Genet. Dev.* **3,** 74–80 (1993).
16. Giraud, C., Winocour, E. & Berns, K. I. Site-specific integration by adeno-associated virus is directed by a cellular DNA sequence. *Proc. Natl Acad. Sci. USA* **91,** 10039–10043 (1994).
17. Kotin, R. M., Linden, R. M. & Berns, K. I. Characterization of a preferred site on human chromosome 19q for integration of adeno-associated virus DNA by non-homologous recombination. *EMBO J.* **11,** 5071–5078 (1992).
18. Cameron, N. E, Cotter, M. A. & Low, P. A. Nerve blood flow in early experimental diabetes in rats: relation to conduction deficits. *Am. J. Physiol.* **261,** E1–E8 (1991).
19. Studier, F. W., Rosenberg, A. H., Dunn, J. J. & Dubendorff, J. W. Use of T7 RNA polymerase to direct expression of cloned genes. *Methods Enzymol.* **185,** 60–89 (1990).
20. Pollet, R. J., Standaert, M. L. & Haase, B. A. Insulin binding to the human lymphocyte receptor. Evaluation of the negative cooperativity model. *J. Biol. Chem.* **252,** 5828–5834 (1977).
21. Roth, J. Assay of peptide hormones using cell receptors: application to insulin and to human growth hormone. *Methods Enzymol.* **37,** 66–82 (1975).
22. Frost, S. C. & Lane, M. D. Evidence for the involvement of vicinal sulfhydryl groups in insulin-activated hexose transport by 3T3-L1 adipocytes. *J. Biol. Chem.* **260,** 2646–2652 (1985).
23. Heath, W. F. *et al.* (A-C-B) human proinsulin, a novel insulin agonist and intermediate in the synthesis of biosynthetic human insulin. *J. Biol. Chem.* **267,** 419–425 (1992).
24. Yoon, J. W., Lesniak, M. A., Fussganger, R. & Notkins, A. L. Genetic differences in susceptibility of pancreatic β-cells to virus-induced diabetes mellitus. *Nature* **264,** 178–180 (1976).
25. Ma, Z. *et al.* Effect of hemoglobin- and Perflubron-based oxygen carriers on common clinical laboratory tests. *Clin. Chem.* **43,** 1732–1737 (1997).
26. Yoon, J. W., Rodrigues, M. M., Currier, C. & Notkins, A. Long-term complications of virus-induced diabetes mellitus in mice. *Nature* **296,** 566–569 (1982).
27. Yoon, J. W. *et al.* Control of autoimmune diabetes in NOD mice by GAD expression or suppression in cells. *Science* **284,** 1183–1187 (1999).
28. Hirasawa, K. Possible role of macrophage-derived soluble mediators in the pathogenesis of EMC virus-induced diabetes in mice. *J. Virol.* **71,** 4024–4031 (1997).

Acknowledgements

We thank R. J. Samulski for providing psub201 and pXX2, A. L. Kyle and K. Clarke for editorial assistance and B. Pinder for artwork. We also thank H. S. Jun for a critical review of the manuscript. J. W. Y. is a Heritage Medical Scientist awardee of the Alberta Heritage Foundation for Medical Research. This work was supported in part by Brain Korea 21 Project.

Correspondence and requests for materials should be addressed to H.C.L. (e-mail: endohclee@yumc.yonsei.ac.kr)

A ubiquitin-like system mediates protein lipidation

Yoshinobu Ichimura*†‡, Takayoshi Kirisako*†‡, Toshifumi Takao§, Yoshinori Satomi§, Yasutsugu Shimonishi§, Naotada Ishihara*, Noboru Mizushima*‖, Isei Tanida¶, Eiki Kominami¶, Mariko Ohsumi#, Takeshi Noda*† & Yoshinori Ohsumi*†

** Department of Cell Biology, National Institute for Basic Biology, 38 Nishigonaka, Myodaijicho, Okazaki 444-8585, Japan*
† Department of Molecular Biomechanics, School of Life Science, The Graduate University for Advanced Studies, Okazaki 444-8585, Japan
§ Institute for Protein Research, Osaka University, Yamadaoka 3-2, Suita, Osaka 565-0871, Japan
‖ PRESTO, Japan Science and Technology Corporation (JST), Kawaguchi 332-0012, Japan
 # Department of Biosciences, High Tech Research Center, Teikyo University of Science and Technology, Yamanashi 409-0193, Japan
¶ Department of Biochemistry, Juntendo University School of Medicine, Tokyo 113-8421, Japan
‡ These authors contributed equally to this work

Autophagy is a dynamic membrane phenomenon for bulk protein degradation in the lysosome/vacuole[1,2]. Apg8/Aut7 is an essential factor for autophagy in yeast[3–5]. We previously found that the carboxy-terminal arginine of nascent Apg8 is removed by Apg4/Aut2 protease, leaving a glycine residue at the C terminus[6]. Apg8 is then converted to a form (Apg8-X) that is tightly bound to the membrane[6]. Here we report a new mode of protein lipidation. Apg8 is covalently conjugated to phosphatidylethanolamine through an amide bond between the C-terminal glycine and the amino group of phosphatidylethanolamine. This lipidation is mediated by a ubiquitination-like system. Apg8 is a ubiquitin-like protein that is activated by an E1 protein, Apg7 (refs 7, 8), and is transferred subsequently to the E2 enzymes Apg3/Aut1 (ref. 9). Apg7 activates two different ubiquitin-like proteins, Apg12 (ref. 10) and Apg8, and assigns them to specific E2 enzymes, Apg10 (ref. 11) and Apg3, respectively. These reactions are necessary for the formation of Apg8-phosphatidylethanolamine. This lipidation has an essential role in membrane dynamics during autophagy[6].

Apg8 was the first molecule found to localize to the intermediate structures of the autophagosome, and is necessary for autophagosome formation[4,5]. Apg8-X behaves like an integral membrane protein, even though Apg8 does not possess a membrane-spanning region[6]. Here we used phase partitioning with Triton X-114 to separate Apg8-X. In wild-type cells, a small amount of Apg8 was detected in the detergent phase—most of it was in the aqueous phase (Fig. 1a). In contrast, Δ*apg7* cells resulted in the exclusive partitioning of Apg8 to the aqueous phase (Fig. 1a). Apg8-X accumulated in Δ*apg4*Δ*apg8* cells expressing Apg8FG (Apg8 lacking the C-terminal arginine)[6], resulting in marked enhancement of detergent phase partitioning (Fig. 1a). These results indicate that Apg8 acquires sufficient hydrophobicity for membrane insertion after the attachment of molecule X.

To assess directly the structure of Apg8-X, we purified it from Δ*apg4*Δ*apg8* cells expressing His_6–Apg8FG. Matrix-assisted laser-desorption ionization time-of-flight mass spectrometry (MALDI–TOFMS) gave two signals at *m*/*z* 14,368 and 15,003 (Fig. 1b). The former value was assigned to the molecule His_6–Apg8FG (14,297) modified with an acrylamide monomer (relative molecular mass (M_r) 71) derived from SDS/polyacrylamide gel electrophoresis (PAGE). The latter was assigned to the His_6–Apg8-X. The difference in molecular mass (635) and hydrophobic nature of Apg8-X suggested that X is a glycerophospholipid. In fact, the His_6–Apg8-